Coupled-View Based Ranking Optimization for Person Re-identification

Mang Ye[1], Jun Chen[1,2], Qingming Leng[3], Chao Liang[1,2], Zheng Wang[1], and Kaimin Sun[4]

[1] National Engineering Research Center for Multimedia Software, School of Computer, Wuhan University, Wuhan, 430072, China
[2] Research Institute of Wuhan University in Shenzhen, China
[3] School of Information Science and Technology, Jiujiang University, China
[4] State Key Laboratory of Information Engineering in Surveying, Mapping, and Remote Sensing, Wuhan University, China
yemang@whu.edu.cn

Abstract. Person re-identification aims to match different persons observed in non-overlapping camera views. Researchers have proposed many person descriptors based on global or local descriptions, while both of them have achieved satisfying matching results, however, their ranking lists usually vary a lot for the same query person. These motivate us to investigate an approach to aggregate them to optimize the original matching results. In this paper, we proposed a coupled-view based ranking optimization method through cross KNN rank aggregation and graph-based re-ranking to revise the original ranking lists. Its core assumption is that the images of the same person should share the similar visual appearance in both global and local views. Extensive experiments on two datasets show the superiority of our proposed method with an average improvement of 20-30% over the state-of-the-art methods at CMC@1.

Keywords: Coupled-view, Ranking optimization, Person re-identification.

1 Introduction

In recent years, the person re-identification problem, namely matching people across disjoint camera views in a multi-camera system, has aroused an increasing interest in computer vision, and multimedia analysis communities [1]. The main challenges in person re-identification can be attributed to the significant visual changes in pose, illumination and viewpoint, making intra-personal variations even larger than that of inter-personal variations [7]. In addition, background clutters and occlusions cause additional difficulties [19].

To address above problems, previous works focus on constructing and selecting various distinctive and stable appearance representations for accurate identity recognition. According to the feature types of those methods, relevant work can be roughly divided into two categories: the global feature based methods [2–5] and the local feature based methods [1, 7, 8, 12, 19]. The global feature

X. He et al. (Eds.): MMM 2015, Part I, LNCS 8935, pp. 105–117, 2015.

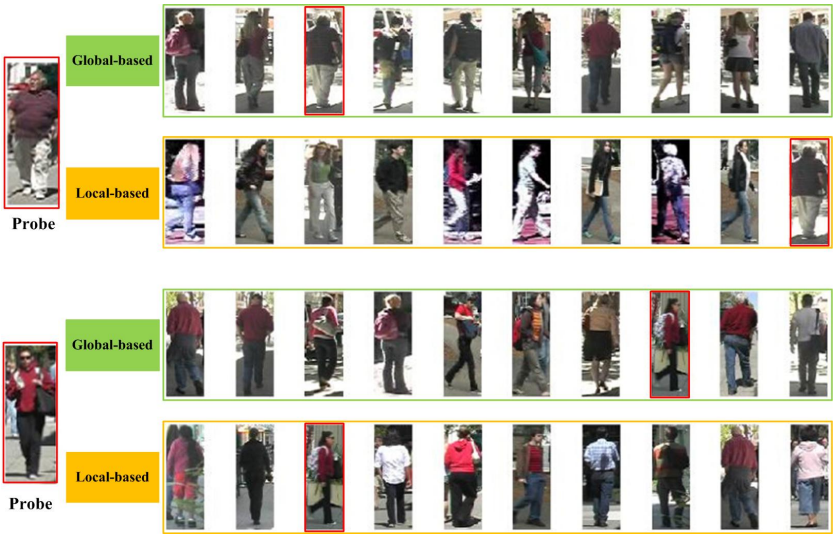

Fig. 1. Person re-identification rank lists based on global and local methods. The red box shows the groundtruth. The global feature based method is achieved by KISSME [5], while the local feature based method is conducted by SDC [7]. Note the ranking difference between the methods while both of them achieved good results.

based methods try to integrally define a global appearance human signature with rich image features and match given reference images with the observations. For example, D. Gray et al. [2] proposed the feature ensemble to deal with viewpoint invariant recognition. To improve the performance, advanced learning techniques are employed for more reliable matching metrics, Kostinger et al. [5] projected the concatenated feature histograms into subspace by PCA to retain their global information for metric learning. The local feature based methods focus on extracting weighted patch-based features to highlight some local regions, which is decisive for constructing discriminative descriptions. For example, N. Gheissari et al. [1] adopted a decomposable triangulated graph to represent person configuration. Zhao et al. [7] extracted distinctive features by unsupervised salience learning to find the salience regions for constructing robust discriminative descriptions. More specially, the global feature based methods delineate overall feature distributions in person images, thus the retrieved candidates often appear alike at a glance but may be irrelevant, while the local feature based methods are powerful in identifying near-duplicate local regions since some local regions may be occluded or conjuncted. The complementary descriptive capability of global and local feature based methods naturally raise the question of how to aggregate them to yield better results.

As reported in existing works, both of these two category methods could achieve a relatively satisfactory results on the public datasets, e.g. VIPeR [21], CUHK01 [22] and etc. However, it's amazing to find that the ranking lists of these

Table 1. The person proportion of different overlapping ratios. The result is achieved by computing the overlapping ratios of top 20 results. Note that most overlapping ratio of the query persons are under a low value, i.e. the ranking lists vary a lot.

Overlapping ratio	0-15%	20-25%	30-45%	50-100%
Person proportion	92.08±2.21	7.59±0.91	0.32±0.15	0

two methods vary greatly. We conduct a preliminary experiment on the famous VIPeR [21] dataset to reveal the ranking difference, achieved by KISSME [5] and SDC [7] shown in Fig. 1. As shown in the figure, the global feature based yield a better result when the person possesses a single overall appearance characteristic, while the local feature based method is better when the person owns some salient local regions. Thus it can be seen that both of them can achieve relatively good results but their ranking lists vary a lot. Further more, an objective statistical data is reported in Table 1, in which the overlapping ratio is computed by the intersection size of the top 20 ranking results achieved by KISSME and SDC methods, respectively. As illustrated in the table, the overlapping ratio of most query persons is below 15%, which further verifies the ranking difference between the global and local methods. Based on these observations, their ranking lists vary a lot while both of them yield decent matching rates. These prompt us to investigate a coupled-view based ranking optimization method based on these two category methods to optimize person re-identification task.

Actually, researchers have proposed several ranking optimization methods [13–15] to revise the original ranking results, which can be categorized into two kinds: interactive relevance feedback methods and automatic re-ranking methods. For interactive relevance feedback, Ali et al [17] employed rank based constraints and convex optimization to efficiently learn the distance metric; Liu et al [14] presented a interactive error-prone post-rank visual search method at the user end. However, the interactive methods need lots of manpower which is not suitable for large scale data scenarios. For automatic re-ranking, Leng et al [13] proposed a automotive bidirectional ranking method based on the content and context similarity, but they ignore the reliability of k-nearest neighbors, and adopted the same query method for the backward re-ranking; Hirzer et al [18] proposed a similar combination method based on covariance descriptors and discriminative model, while the complementary of the two aspects is too far-fetched. In other words, existing ranking optimization methods are merely taking a single view into account. The ranking aggregation of these two category methods is seldom investigated in person re-identification.

In this paper, we proposed a novel coupled-view based rank optimization method for person re-identification based on these two complementary lines. A latent assumption is that two person images are more likely to be the same person if they share similar appearance in both global feature based and local feature based views. In particular, if a person image appeared in top-k ranking list in both global and local views, it will be more likely to be the correct match of the query image. At this point, we propose a KNN rank aggregation method by

crossed-view based requery. Moreover, motivated by the relationships in social network, good friends are always trend to have more common friends [16], i.e., images captured from the same person will have more mutual k-nearest neighbors than that of different persons. Therefore, we can revise the original ranking lists by combining the nearest neighbours network similarity of the global and local feature based results. Based on this, we conduct a graph-based reranking method by constructing a two-layer complementary graph.

The main contribution of the proposed coupled-view based ranking optimization approach can be summarized as follows: (1) rank aggregation is firstly conducted in person re-identification task; (2) it presents a more reasonable combination of two category complementary methods; (3) the approach can be easily transplanted to other methods. And we have validated our approach on two public datasets, the VIPeR [21] and CUHK01 [22]. The experimental results illustrate that our method outperforms all the existing ranking optimization methods and most of the state-of-art methods.

2 Our Approach

2.1 Overview

These two category methods demonstrate distinct strengths in finding visually similar images but their ranking lists vary a lot, and the complementary descriptive capability of global and local methods makes our ranking optimization work valid. To aggregate the ranking lists achieved by different category methods, the critical issue is how to automatically measure and compare their qualities. However, the similarity scores of candidates vary largely among different queries, moreover, the similarity metrics vary a lot for different methods, all these exacerbate the directly combination difficulty of two methods. Despite these, there are many researches focus on solving this problem. More broadly, in general image retrieval, Zhang et al [20] proposed a graph fusion method, they measured the consistency among the top candidates returned by one retrieval method as the retrieval quality specific to one query, it may rely too much on the assumption that the groundtruths of the query image are always in the top k candidates which is not applied to person re-identification task, while there is only one correct match in the re-identification task [9], i.e. the top k results contain too much false matchings, it may lead to the algorithm difficult to converged and may aggravate the noise affection and increase false matching after several iterations.

The overall framework of our method is shown in Fig. 2. In order to enhance the complementarity of the two category methods, we combine them in all steps of our method. Differ to existing methods [20], we adopt conjunct neighbours in both global and local views to generate more reliable k_c nearest neighbours, instead of top k candidates directly, the sketch is shown in Fig.2(a). After getting the original ranking lists, the k_c nearest neighbours are treated as new probes to query in the original gallery set, named backward requery. More specially, to enhance the complementary of two methods, the crossed backward requery

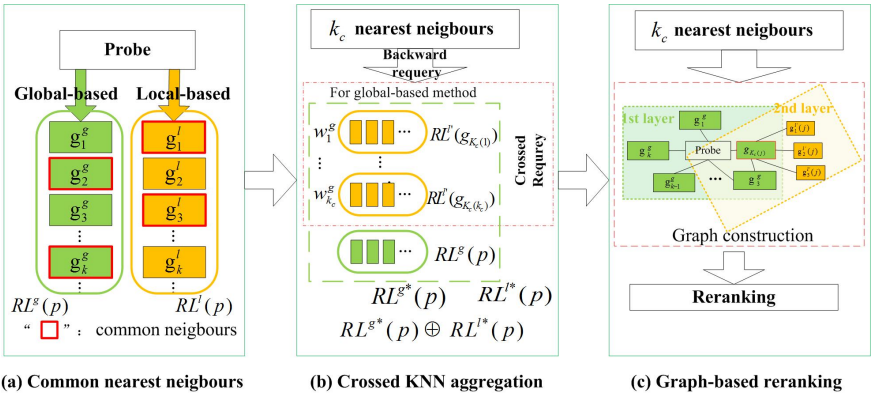

Fig. 2. The Framework of our method.(a) Common nearest neighbours; (b) Crossed KNN aggregation; (c) Graph-based reranking. Note that the superscripts denote different methods. The green and orange depict the two different methods. While the rectangle represents a person image and the rounded rectangles denote different ranking lists.

is conducted, i.e., the local-based methods is adopted for requery to revise the original global-based methods and vice versa. After that, weighted aggregation of the multi-ranking lists is introduced as shown in Fig.2(b). While the whole ranking list is revised by the crossed KNN rank aggregation, further more, the more reliable k_c neighbours are reranked by constructing a two-layer graph about the k_c common neighbours based on the two methods, the Jaccard similarity coefficient of two neighborhood images is computed, defined as graph-based reranking illustrated in Fig.2(c). The details are discussed in the following.

2.2 Common Nearest Neighbours

For the convenience of following discussion, we consider the probe person image as p and a gallery set as $G = \{g_i \mid i = 1, 2, ...n\}$, while n is the number of images in gallery set. And the global feature based method we mark it with superscript g, while local feature based method with l. We firstly get two original ranking lists achieved by two methods of query p, denote as $RL^g(p)$ and $RL^l(p)$, the k nearest neighbours of each method denote as $RL^g_k(p)$ and $RL^l_k(p)$. To get the more reliable nearest neighbours, we define their common nearest neighbours $G_{K_c}(p) = \{g_{K_c(j)} \mid j = 1, 2, ...k_c, k_c \leq k\}$as the true neighbours of image p, k_c is the number of the common nearest neighbours, which is depicted in Fig.2(a):

$$\{G_{K_c}(p)\} = \{RL^g_k(p)\} \cap \{RL^g_k(p)\} \tag{1}$$

2.3 Crossed KNN Rank Aggregation

While we have gotten more reliable k-nearest neighbours, we choose the common nearest neighbours $G_{K_c}(p)$ for backward requery, i.e. we treat the each $g_{K_c(j)}$

in $G_{K_c}(p)$ as a new probe to search in the original gallery set. To enhance the complement of global and local methods, we adopt the crossed-view based re-query, that is to say, we revise the original global feature based ranking lists $RL^g(p)$ with local feature based methods for requery and vice versa, which is depicted in Fig.2(b). For the backward requery , $(k_c + 1)$ ranking lists for each category method are achieved, i.e. one original ranking lists and k_c crossed re-query ranking lists. For better presentation, we treat it as an example, of which the original ranking list is achieved by global feature based method and the local feature based method for backward requery.

$$RL^{g^*}(p) = \{RL^g(p), \quad RL^{l'}(g_{K_c(1)}), RL^{l'}(g_{K_c(2)}), \ldots, RL^{l'}(g_{K_c(k_c)})\} \tag{2}$$

For better combination, we aggregate the ranking lists weighting by their context similarity, which represents their neighbours similarity between the query and the probe, $N_k^g(p)$ represents the k-nearset neighbours of the original ranking list and $N_k^{l'}(g_{K_c(j)})$ for the crossed backward requery neighbours:

$$w^g(g_{K_c(j)}) = \frac{\left|N_k^g(p) \cap N_k^{l'}(g_{K_c(j)})\right|}{k} \tag{3}$$

After computing the context similarity, the revised ranking lists of global feature based method, i.e. the eq.(2,3) can be converted to:

$$RL^{g^*}(p) = RL^g(p) + \sum_{j=1}^{k_c} w^g(g_{K_c(j)}) * RL^{l'}(g_{K_c(j)}) \tag{4}$$

Similarly, $RL^{l^*}(p)$ can be achieved by crossed requery, and the final aggregation can be depicted as:

$$Rank^*(p) = \alpha RL^{g^*}(p) + (1 - \alpha) RL^{l^*}(p) \tag{5}$$

where α denote the weighting parameter, we set it $\alpha = 0.8$ in this paper.

2.4 Graph-Based Re-ranking

By the crossed KNN rank aggregation, the entire ranking list is revised. While the k_c common nearest neighbours are more likely to be the correct match, further optimization of the local ranking orders is necessary, a graph-based re-ranking method is proposed. Denote the probe image as p, and $G_{K_c(p)}$ represents their common nearest neighbors for both global and local feature methods.

For each query and each common neighbour $g_{K_c(j)}$, we construct a weighted undirected graph $Graph =< G, E, w >$, the center is the query while the nodes are the neighbour images. As shown in Fig.2(c), for the green part, N_k^g denotes the forward ranking neighbours of probe image received by global-based method, while the orange part $N_k^{l'}$ expresses the backward requry neighbours of $g_{K_c(j)}$,

they are linked by an edge $(p, g_{K_c(j)}) \in E$ if they are common neighbors of two layer graphs. Note that for the second layer of the graph, we adopt the other method differ to the first layer to enhance the complementarity. The revised similarity of p and $g_{K_c(j)}$ is defined as the Jaccard similarity coefficient between the neighborhoods of p and $g_{K_c(j)}$:

$$Sim(p, g_{K_c(j)}) = w(p, g_{K_c(j)}) \frac{\left| N_k^g(p) \cap N_k^{l'}(g_{K_c(j)}) \right|}{\left| N_k^g(p) \cup N_k^{l'}(g_{K_c(j)}) \right|} \tag{6}$$

where $|\cdot|$ denotes the cardinality and $w(p, g_{K_c(j)})$ is a weighting coefficient related to the original rank in $G_{K_c}(p)$, we define it as an decay factor, $rank(g_{K_c(j)}, G_{K_c}(p))$ represents the rank of $g_{K_c(j)}$ in $G_{K_c}(p)$.

$$w(p, g_{K_c(j)}) = {w_0}^{rank(g_{K_c(j)}, G_{K_c}(p))} \tag{7}$$

3 Experiments

3.1 Datasets and Evaluation Protocol

We evaluate our method on two publicly available datasets, the VIPeR dataset [21] and the CUHK01 dataset [22], as for their low image resolution, illuminations, poses and viewpoints variations, which are close to practical surveillance scene. Further more, the two datasets are the largest person re-identification datasets while much more person images are contained. VIPeR is the first dataset that mainly considering the influence of viewpoint change, and it is widely used for evaluating person re-identification methods. CUHK01 dataset get more attentions recently as for its huge number and higher resolution which is more suitable to verify the effectiveness of person re-identification approaches. All the quantitative results are exhibited in standard Cumulated Matching Characteristics (CMC) curves [10].

Following the evaluation protocol described by many predecessors, *i.e.*, we randomly partition the dataset into two even parts, 50% for learning and 50% for testing, without overlap on person identities. All the images from Camera View A are treated as probes while those from Camera View B as gallery set. For each probe image, there is another person image matched in the gallery set, and the rank of correct match is achieved. Rank-k recognition rate is the expectation of finding the correct match within the first k ranks, and the cumulated values of recognition rate at all ranks is recorded as one-trial CMC result. For two different methods, we adopt the same configuration for experiments at each trial to get the ranking lists. Especially, we adopted KISSME [5] as the global feature based method and SDC [7] as the local feature based method. To achieve stable statistics, we looped the evaluation procedure 10 times. We set the parameter top k results as $k = 30$, and the decay factor $w_0 = 0.9$.

3.2 VIPeR Dataset

The VIPeR dataset contains 632 person image pairs captured from two different static camera views in outdoor academic environment. The dataset is challenging due to the viewpoint change of most image pairs is lager than 90 degrees, and with obvious illumination change. All the images are normalized to 128×48 for experiments. The experimental results obtained is shown in Fig. 3, while the Our_RA denotes the crossed KNN rank aggregation step described in Section2.3, and Our_RRA for the graph-based reranking after aggregation, while illustrative results are shown in Fig. 6. Moreover, in Table 2 we compare the performance of our method in the range of the first 25 ranks to existing rank optimization methods and the state-of-the-art methods.

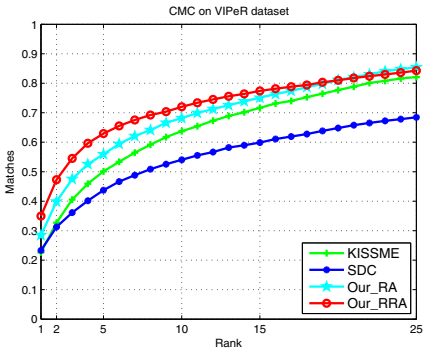

Fig. 3. Performance on the VIPeR dataset. Our approach: Our_RR and Our_RRA based on KISSME [5] and SDC [7].

As can be seen, our approach has huge promotion compared with the baseline global and local methods for both rank aggregation and graph-based reranking methods, more specially, it has nearly 55% improvement at rank 1 for graph-based reranking, and 30% at rank 5. In particular, rank 1 matching rate is around 35% for graph-based reranking and 28% for crossed KNN rank aggregation method only. Further more, compared to existing ranking optimization methods, our results are still more satisfactory, versus 24% for bidirectional ranking [13] and 19% for reranking SB [15]. The results show the efficiency of coupled-view based ranking optimization, while the single-view optimization is limited. The improvement of our approach is due to two aspects: First, we consider both the global similarity and the local similarity which can help us to get more reliable nearest neighbours for rank aggregation, optimize the results by aggregate the different weights ranking lists via the original ranking score; Second, constructing graph by two reciprocal layer with more reliable nearest neighbours give full expression to the combination of global and local feature based methods.

Moreover, comparing to existing state-of-art methods, ELF [2], SDALF [3], PCCA [6], PRDC [4] and SalMatch [19] as shown in Table 2, our results owns more outstanding performance than both metric learning methods and description-based methods in VIPeR dataset. These experimental fact shows the superiority of our methods.

Table 2. VIPeR dataset: top ranked matching rates in [%] with 316 persons

Methods	$r = 1$	$r = 2$	$r = 5$	$r = 10$	$r = 15$	$r = 25$
Our_RA	28.48	39.87	55.92	68.20	75.06	**85.41**
Our_RRA	**34.97**	**47.28**	**62.94**	**72.03**	**77.41**	85.18
SB [15]	19.32	50.70	63.37	71.28	81.18	
Bi-ranking [13]	24.57	35.28	53.38	65.18	73.32	84.27
ELF [2]	12.08	17.00	31.28	41.00	54.00	65.00
SDALF [3]	19.87	25.20	38.89	49.37	58.22	70.00
PRDC [4]	15.66	22.80	38.42	53.86	64.00	72.78
PCCA [6]	19.27	29.10	48.89	64.91	72.48	82.78
KISSME [5]	22.63	32.72	50.13	63.73	71.65	82.12
SDC [7][a]	23.32	31.27	43.73	54.05	59.87	68.45
SalMatch [19]	30.16	39.28	52.00	65.00	74.00	*

[a] It differs to [7], because they removed the complicated 98 person pairs, while we retain them as many other papers.

To further verify the availability of our method, we conduct another experiment on VIPeR shown in Fig. 4. The global feature based method we adopted is SDALF[1] [3], and the local feature based method we aopted is LDFV[2] [12]. Thus can be seen, the optimization result is satisfactory.

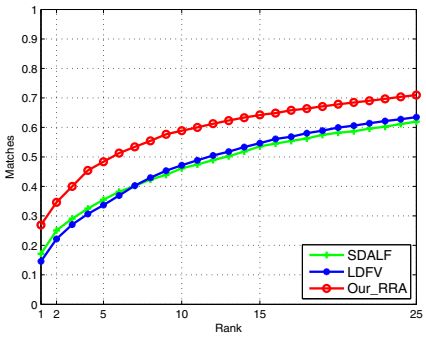

Fig. 4. Performance on the VIPeR dataset. Our approach based on SDALF [3] and LDFV [12].

[1] It is available at
`http://www.lorisbazzani.info/code-datasets/sdalf- descriptor/`
[2] It is available at `http://vipl.ict.ac.cn/members/bpma`

3.3 CUHK01 Dataset

The CUHK01 dataset is also obtained from two disjoint camera views in an outdoor campus environment. And it contains 971 persons much more than that of VIPeR which can be more convincible for experiments, and each person has two images in each camera. The person images in camera A are mostly captured by frontal view or back views while camera B captures the side views. All the images are normalized to 160×60 for experiments.

The experimental results based on KISSME [5] and SDC [7] are shown in Fig. 5. The results show our improvement at rank 1 is about 35%, while improved 20% at rank 10, it makes the efficiency of our method more convincible. And more comparison to existing state-of-the-art methods is shown in Table 3, since the dataset is newly reported and experiments are seldom conducted, therefore, the results are mostly from [19]. Apparently, our coupled-view ranking optimization method outperforms the existing approaches, and similar conclusions as shown in VIPeR dataset can be drawn from the comparisons.

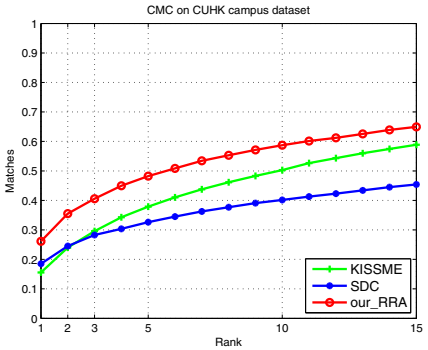

Fig. 5. Performance on the CUHK01 dataset

Table 3. CUHK01 dataset: top ranked matching rates in [%] with 485 persons

Methods	$r = 1$	$r = 2$	$r = 3$	$r = 5$	$r = 10$	$r = 15$
SDALF [3]	9.90	13.58	18.00	22.00	30.20	35.00
KISSME [5]	15.57	24.00	29.57	37.90	50.29	58.89
SDC [7]	18.52	24.52	28.29	32.62	40.14	45.42
LMNN [22]	13.45	20.15	24.50	31.00	41.50	49.00
ITML [22]	15.98	23.00	28.00	35.50	45.50	54.00
SalMatch [19]	**28.45**	**36.00**	40.00	46.00	55.50	63.00
Our_RRA	26.37	34.74	**40.66**	**48.76**	**60.58**	**68.40**

Fig. 6. Two descriptive re-identification results from VIPeR dataset. Top-10 candidates are shown for the optimization results, the red box represents the groundtruth.

4 Conclusion

In this paper, we address the ranking optimization approaches of the person re-identification problem, a novel and efficient coupled-view based ranking optimization method based on local and global feature method is conducted. The main idea is: the two images of the same person should share similar appearance in both global-based view and local-based view, the crossed KNN rank aggregation is conducted. Furthermore, motivated by the ideology in social network, if the two image share similar reciprocal neighbours, they are more likely to be the same person. Specially, constructing complementary graphs to illustrate the relations and improve the re-identification results. Extensive experiments compared to the original baseline methods and existing state-of-art methods on two publicly datasets have validated the effectiveness of our proposed method.

Acknowledgement. The research was supported by the National Nature Science Foundation of China (61303114, 61231015, 61170023), the Specialized Research Fund for the Doctoral Program of Higher Education (20130141120024), the Technology Research Project of Ministry of Public Security (2014JSYJA016), the Fundamental Research Funds for the Central Universities (2042014kf0250), the China Postdoctoral Science Foundation funded project (2013M530350), the major Science and Technology Innovation Plan of Hubei Province (2013AAA020), the Key Technology R&D Program of Wuhan (2013030409020109), the Guangdong-Hongkong Key Domain Break-through Project of China (2012A090200007), and the Special Project on the Integration of Industry, Education and Research of Guangdong Province (2011B090400601).

References

[1] Gheissari, N., Sebastian, T.B., et al.: Person re-identification using spatiotemporal appearance. In: Computer Vision and Pattern Recognition (CVPR), pp. 1528–1535 (2006)

[2] Gray, D., Tao, H.: Viewpoint invariant pedestrian recognition with an ensemble of localized features. In: Forsyth, D., Torr, P., Zisserman, A. (eds.) ECCV 2008, Part I. LNCS, vol. 5302, pp. 262–275. Springer, Heidelberg (2008)

[3] Farenzena, M., Bazzani, L., Perina, A., et al.: Person re-identification by symmetry-driven accumulation of local features. In: Computer Vision and Pattern Recognition (CVPR), pp. 2360–2367 (2010)

[4] Zheng, W.S., Gong, S., Xiang, T.: Person re-identification by probabilistic relative distance comparison. In: Computer Vision and Pattern Recognition (CVPR), pp. 649–656 (2011)

[5] Kostinger, M., Hirzer, M., Wohlhart, P., et al.: Large scale metric learning from equivalence constraints. In: Computer Vision and Pattern Recognition (CVPR), pp. 2288–2295 (2012)

[6] Mignon, A., Jurie, F.: PCCA: A new approach for distance learning from sparse pairwise constraints. In: Computer Vision and Pattern Recognition (CVPR), pp. 2666–2672 (2012)

[7] Zhao, R., Ouyang, W., Wang, X.: Unsupervised salience learning for person re-identification. In: Computer Vision and Pattern Recognition (CVPR), pp. 3586–3593 (2013)

[8] Xu, Y., Lin, L., Zheng, W.S., et al.: Human re-identification by matching compositional template with cluster sampling. In: International Conference on Computer Vision (ICCV), pp. 3152–3159 (2013)

[9] Javed, O., Shafique, K., Shah, M.: Appearance modeling for tracking in multiple non-overlapping cameras. In: Computer Vision and Pattern Recognition (CVPR), vol. 2, pp. 26–33 (2005)

[10] Wang, X., Doretto, G., Sebastian, T., et al.: Shape and appearance context modeling. In: International Conference on Computer Vision (ICCV), pp. 1–8 (2007)

[11] Hirzer, M., Roth, P.M., Köstinger, M., Bischof, H.: Relaxed pairwise learned metric for person re-identification. In: Fitzgibbon, A., Lazebnik, S., Perona, P., Sato, Y., Schmid, C. (eds.) ECCV 2012, Part VI. LNCS, vol. 7577, pp. 780–793. Springer, Heidelberg (2012)

[12] Ma, B., Su, Y., Jurie, F.: Local descriptors encoded by fisher vectors for person re-identification. In: European Conference on Computer Vision Workshops and Demonstrations (ECCV Workshop), pp. 413–422 (2012)
[13] Leng, Q., Hu, R., Liang, C., et al.: Bidirectional ranking for person re-identification. In: International Conference on Multimedia and Expo (ICME), pp. 1–6 (2013)
[14] Liu, C., Loy, C.C., Gong, S., et al.: POP: Person re-identification post-rank optimisation. In: International Conference on Computer Vision (ICCV), pp. 441–448 (2013)
[15] An, L., Chen, X., Kafai, M., et al.: Improving person re-identification by soft biometrics based reranking. In: International Conference on Distributed Smart Cameras (ICDSC), pp. 1–6 (2013)
[16] Leng, Q., Hu, R., Liang, C., et al.: Person re-identification with content and context re-ranking. In: Multimedia Tools and Applications, pp. 1–26 (2014)
[17] Ali, S., Javed, O., Haering, N., et al.: Interactive retrieval of targets for wide area surveillance. In: International Conference on Multimedia (MM), pp. 895–898 (2010)
[18] Hirzer, M., Beleznai, C., Roth, P.M., et al.: Person re-identification by descriptive and discriminative classification. In: Image Analysis (IA), pp. 91–102 (2011)
[19] Zhao, R., Ouyang, W., Wang, X.: Person re-identification by salience matching. In: International Conference on Computer Vision (ICCV), pp. 2528–2535 (2013)
[20] Zhang, S., Yang, M., Cour, T., et al.: Query specific fusion for image retrieval. In: European Conference on Computer Vision(ECCV), pp. 660–673 (2012)
[21] Gray, D., Brennan, S., Tao, H.: Evaluating appearance models for recognition, reacquisition, and tracking. In: IEEE International Workshop on Performance Evaluation of Tracking and Surveillance (2007)
[22] Li, W., Wang, X.: Locally aligned feature transforms across views. In: Computer Vision and Pattern Recognition (CVPR), pp. 3594–3601 (2013)